JCAMECH

Vol. 51, No. 1, June 2020, pp 199-212
DOI: 10.22059/jcamech.2018.247631.218

Attractor Based Analysis of Centrally Cracked Plate Subjected to Chaotic Excitation

*Sina Jalili, Alireza Daneshmehr**

Mechanical Engineering School, University of Tehran, Tehran, Iran

ARTICLE INFO

Article history:
Received: 9 December 2017
Accepted: 10 May 2018

Keywords:
Crack
chaotic
nonlinear dynamics
plate
prediction error

ABSTRACT

The presence of part-through cracks with limited length is one of the prevalent defects in the plate structures. Due to the slight effect of this type of damages on the frequency response of the plates, conventional vibration-based damage assessment could be a challenging task. In this study for the first time, a recently developed state-space method which is based on the chaotic excitation is implemented and nonlinear prediction error (NPE) is proposed as a geometrical feature to analyze the chaotic attractor of a centrally cracked plate. For this purpose using line spring method (LSM) a nonlinear multi-degree of freedom model of part through cracked rectangular plate is developed. Tuning of Lorenz type chaotic signal is conducted by crossing of the Lyapunov exponents' spectrums of nonlinear model of the plate and chaotic signal and in the next step by varying the tuning parameter to find a span in which a tangible sensitivity in the NPE could be observable. Damage characteristics such as length, depth and angle of crack are altered and variation of proposed feature is scrutinized. Results show that by implementation of the tuned chaotic signal, tangible sensitivity and also near to monotonic behavior of NPE versus damage intensity are achievable. Finally, the superiority of the proposed method is examined through the comparison with the frequency-based method.

1. Introduction

Geometrical discontinuities such as cracks in shell and plate structures which play the main role of protecting in engineering structures can lead to catastrophic consequences. Study on the vibrational response of structures can help to reveal the malfunctions in the structures. However, due to slighter effect of part through cracks on the dynamic response of thin walled structures they may be a challenge for Vibrational Structural Health Monitoring (VSHM). In addition, three-dimensional nature of part through cracked shells and structures makes modeling and analysis of this type of problems a tedious task. Therefore, limited number of researchers concerned plate and thin walled structures containing cracks. Rice and Levy [1] conducted the first work aimed to reduce the three dimensional problem of part through crack in a plate to two dimensional. They developed line spring method (LSM) to predict stress intensity factors in bending and tension modes by combination of Kirchhoff plate theory with two-dimensional edge cracked medium. An extension of work of Rice and Levy[1] for antisymmetric loading condition which causes the crack to get excited in II and III modes was carried out by Joseph and Erdogan [2]. Wen and Zhixe [3] made some modifications to accommodate crack location parameter into the LSM. Effect of crack inclination under biaxial stress state was investigated by Zeng and Dai [4]. Problem of through crack presence in shells under skew-symmetric loading was studied by Delale [5]. A Green function solution for crack and anti-rack problem in thin plates is offered by Cheng and Reddy[6]. Most of the mentioned researches concerned the static loading and aimed estimation of the crack stress intensity factor and a limited number of researches have been devoted to dynamic response of cracked plate. Israr et al. [7] fulfilled the first study on the dynamic characteristics of a cracked plate by implementation of LSM. In this work, a nonlinear partial differential equation was developed

* Corresponding Author: daneshmehr@ut.ac.ir

by combination of Berger formulation [8] and LSM, for a centrally located crack which was parallel with one of main axis of rectangular plate. Later Ismail and Cartmell [9] extended the work of Israr et al. [7] to capture the effect of crack orientation on the dynamic response of plate. They exploited the stress and moments transformation relations to modify the mathematical equations, accordingly. Initial proposed problem was investigated further by Bose and Mohanty[10] to take the effect of crack location into account. By implementation of modified line spring method (MLSM) of [3]and[9] , they developed an analytical model which covered the effect of crack orientation and location on the governing dynamic equation. Li et al. [11] considered the vibrational energy flow and wave propagation characteristics of over-all part-through cracked plate using LSM model. Linear and nonlinear frequency response of cracked plate was the main concern of formerly referred works. Most of results in the previous researches showed that effect of a part-through crack with limited length has negligible effect on the frequency response of plates which hinders conventional vibrational based procedures to assess the crack effect. In recent years, time-series based procedures developed which may be used to cover the shortages of frequency based method. Kuroiwa and Iemura[12] used Auto-Regressive (AR) and Auto-regressive with eXogenous inputs (ARX) statistical models to make a time series based analysis which was implemented on a 5-story steel frame model. Trendafilova and Manoach[13] by inspection of the changes in geometrical features of state space dynamic response of a damaged plate proposed a vibration based health monitoring scheme. Figueiredo et al. [14] proposed a nonlinear time-series procedure which utilized Autoregressive modeling to detect damages under variable operational conditions. Use of chaotic signal as a interrogator which developed in recent years was proposed by Todd et al. [15].Their work considered state space framework and suggested that local attractor variance ratio (ALAVR) to be a damage sensitive feature and examined the proposed method on a FEM model of a thin aluminum cantilever beam. In other research, Nichols et al. [16] investigated variation of an attractor based property called prediction error as a damage sensitive feature on a simplified nonlinear model. Ryue and White [17] implemented chaotic excitation to inspect the correlation dimension and Hausdorff distant as features in a cracked beams's state space response. Epureanu et al. [18] proposed a nonlinear dynamic based enhanced sensitivity scheme based on the feedback from structure response under chaotic excitation. Torkamani et al. [19] investigated the hyperchaotic probing of damaged structures and utilized prediction error as a feature and found out that hyperchaotic interrogation could enhance sensitivity of proposed feature to damage alteration in a tangible manner. It is not necessary to note that there are considerable researches which deal with the vibration of intact thin walled structures. Flat plates are among the structures that numerous studies devoted to the study of their linear and nonlinear responses [20], [21]. Researchers also are interested in the stability behavior of cracked plates. Shishesaz et al. [22] studied the buckling of centrally defected composite plates under the in-plane compression loading.

2. In this study, for the first time, the nonlinear prediction error is proposed as a damage sensitive feature to investigate the sensitivity of chaotic attractor for the health monitoring of part-through cracked plates. This feature deals with the fractal and geometrical attributes of chaotic attractors. Present research, conducts a comprehensive study on the chaotic interrogation of cracked plates. For this purpose, a nonlinear multi-degree of freedom model of part-through cracked plate is developed by MLSM procedure. Evaluation of feasibility of the proposed model in time-series domain was examined through comparison with a detailed three-dimensional FE model. Nonlinear auto prediction error (NAPE) as a geometrical metering tool for comparison of chaotic attractors is proposed to be a damage sensitive feature. After establishment of the nonlinear model, Lorenz type chaotic signal was implemented to excite the nonlinear model of cracked plate. To confirm that the chaotic signal Lyapunov's dimension will be altered via passing from the model, crossing of Lyapunov exponents' spectrum (LEs) of cracked plate model with the interrogator signal is examined. In order to set a better tuning, effect of change of tuning parameter on the NAPE is surveyed to find a span within proposed feature reaches to a tangible sensitivity. By using of tuned chaotic signal, effect of the crack properties' alteration e.g. crack's length, orientation and depth on the variation of mentioned feature is investigated.

2. Problem Description

The rectangular plate which is considered in this study contains a single part-through crack located in center of the plate (Fig.1). Plate dimensions are l_1 and l_2 in x and y directions and crack length is 2a. Crack makes an angle θ with x direction. Crack has a depth ratio of ζ which is defined as the ratio of crack depth to the plate thickness (h). The plate is constructed from a linear elastic isotropic material with modulus of elasticity, E, Poisson ratio of ν and density of ρ . Moreover, the plate subjected to an excitation force, F which acts in (x0, y0) location.

In carrying out this project, epoxy resin was used as matrix material, while fibre glass and talc were used as filler for the production of the thermoset composite.

For the purpose of this experiment, Talc was sieved into average particle sizes of 75 µm and 106 µm using a mechanical sieve. The fiber glass was cut into short pieces of approximately equal length, with an aspect ratio of 0.08. The mold was coated in Poly Vinyl Alcohol (mold release agent) and left to dry before pouring the resin mixture.

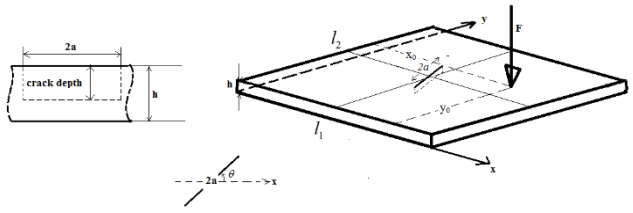

Figure 1. Center part-through cracked plate, geometrical configuration

$$
\begin{aligned}
&D\left(\frac{\partial^4 w}{\partial x^4}+2\frac{\partial^4 w}{\partial x^2\partial y^2}+\frac{\partial^4 w}{\partial y^4}\right)= \\
&-\rho h\frac{\partial^2 w}{\partial t^2}+\frac{\partial^2 \bar{M}_x}{\partial x^2}+(N_x+\bar{N}_x) \\
&\frac{\partial^2 w}{\partial x^2}+\frac{\partial^2 \bar{M}_y}{\partial y^2}(N_y+\bar{N}_y)\frac{\partial^2 w}{\partial y^2} \\
&+2\frac{\partial^2 \bar{M}_{xy}}{\partial x\partial y}+2(N_{xy}+\bar{N}_{xy}) \\
&\frac{\partial^2 w}{\partial x\partial y}+F*\delta(x-x_0)\delta(y-y_0)
\end{aligned}
\qquad (1)
$$

Where $D=\frac{Eh^3}{12(1-\nu^2)}$ is flexural rigidity of the plate and δ denotes to the Dirac delta function. $N_x, N_y, N_{xy}=N_{yx}$ are the $i=x,y$ will denote to the net in-plane in x and y directions. $M_x, M_y, M_{xy}=M_{yx}$ are bending moments per unit length and $\bar{M}_x, \bar{M}_y, \bar{M}_{xy}=\bar{M}_{yx}$ are presented due to the introduction of crack into plate. By considering terms with subscript *xy*, effect of angled crack can be taken into account. By introduction of non-dimensional coordinates, $\xi=\frac{x}{l_1}$, $\eta=\frac{y}{l_2}$, and also plate aspect ratio, $\phi=\frac{l_2}{l_1}$, equation (1) can be recast[10]:

$$\frac{\partial^4 w}{\partial\xi^4}+2\frac{\partial^4 w}{\partial\xi^2\partial\eta^2}+\frac{\partial^4 w}{\partial\eta^4}= \frac{-\rho h}{D}\phi^4 l_1^4\frac{\partial^2 w}{\partial t^2}+\frac{1}{Dl_1^2}\frac{\partial^2\bar{M}_x}{\partial\xi^2}+ \frac{\phi^4 l_1^2(N_x+\bar{N}_x)}{D}\frac{\partial^2 w}{\partial\xi^2}+\frac{l_2^2}{D}\frac{\partial^2\bar{M}_y}{\partial\eta^2} +\frac{\phi^2(N_y+\bar{N}_y)l_1^2}{D}\frac{\partial^2 w}{\partial\eta^2}+\frac{2l_2^2\phi}{D}\frac{\partial^2\bar{M}_{xy}}{\partial\xi\partial\eta} +\frac{2l_1^2\phi^3}{D}(N_{xy}+\bar{N}_{xy})\frac{\partial^2 w}{\partial\xi\partial\eta}+ \frac{\phi^4 l_1^4}{D}F*\delta(\xi-\xi_0)\delta(\eta-\eta_0) \tag{2}$$

In line spring method which was firstly offered by Rice and Levy[1], an approximate relationship between the crack tip stresses and far field stresses is introduced. By implementation of LSM, the purely three dimensional problem of part-through crack in a thin plate reduced to a two dimensional one. Using this theory, Israr et al. [7] conducted vibration analysis of a plate which crack located in the center of the plate where crack orientation was parallel to one of x or y directions. Assume that crack is located in an infinite plate where far-field tensile, bending and in –plane shear stresses are acting as illustrated in Figure 2. By plane transformation of stresses to the p-q plane, resulting stresses will be rewritten as:

$$\sigma_p=\frac{\sigma_{xx}+\sigma_{yy}}{2}+\frac{\sigma_{xx}-\sigma_{yy}}{2}\cos(2\theta)+\sigma_{xy}\sin(2\theta)$$
$$\sigma_q=\frac{\sigma_{xx}+\sigma_{yy}}{2}-\frac{\sigma_{xx}-\sigma_{yy}}{2}\cos(2\theta)-\sigma_{xy}\sin(2\theta) \tag{3}$$
$$\sigma_{pq}=-\frac{\sigma_{xx}-\sigma_{yy}}{2}\sin(2\theta)+\sigma_{xy}\cos(2\theta)$$

And also this transformation can be applied on moments:

$$m_p=\frac{m_{xx}+m_{yy}}{2}-\frac{m_{xx}-m_{yy}}{2}\cos(2\theta)-m_{xy}\sin(2\theta)$$
$$m_q=\frac{m_{xx}+m_{yy}}{2}+\frac{m_{xx}-m_{yy}}{2}\cos(2\theta)+m_{xy}\sin(2\theta) \tag{4}$$
$$m_{pq}=-\frac{m_{xx}-m_{yy}}{2}\sin(2\theta)+m_{xy}\cos(2\theta)$$

in-plane forces of an intact plate from which in-plane negative forces $\bar{N}_x, \bar{N}_y, \bar{N}_{xy}=\bar{N}_{yx}$ are subtracted due to presence of the crack. Therefore, summation of $N_i+\bar{N}_i$,

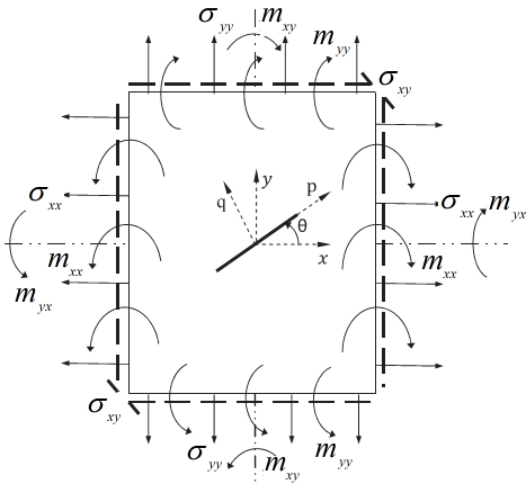

Figure 2. Crack located in an infinite plate subjected to far distance forces and moments.

By above transformation, problem can be rewritten in new plane (p-q), where tensile, bending stresses, shear and twisting stresses are applied on a horizontally oriented crack. For transformed problem, effect of un-cracked ligament is represented by springs which will apply forces and moments on a virtual through crack faces. In other word, by application of these springs a through crack problem would play the role of a part-through one. N_n

In the line spring method, a part through crack mouth opening in normal direction which is under action of far-field tensile stresses σ_p, σ_q and tensile force of is expressed as:

$$\bar{\delta}_n=\frac{4a}{E}(\sigma_q-\sigma_t) \tag{5}$$

where $\sigma_t=\frac{N_n}{h}$. Rotation in the normal direction due to the action of bending moments is expressed as:

$$\bar{\theta}_n=\frac{8(1+\nu)a}{(3+\nu)Eh}(m_p-\sigma_b) \tag{6}$$

In which, $\sigma_b=\frac{6M_n}{h^2}$. Similar to crack mouth normal openings, tangential displacements due to action of tangential stress σ_{pq} and remote force N_t, is:

$$\bar{\delta}_t=\frac{4a}{E}(\sigma_{pq}-\tau_t) \tag{7}$$

Where $\tau_t=\frac{N_t}{h}$. Also, rotation of crack edges in response of application of twisting moment, M_t and remote twisting stress m_{pq}, can be expressed as:

$$\bar{\theta}_t=\frac{8a}{Eh}(m_{pq}-\tau_b) \tag{8}$$

where $\tau_b=\frac{6M_t}{h^2}$. By introduction of dimensionless terms, $\gamma=\frac{h}{l_1}$, $\Gamma=\frac{a}{l_1}$ and using the procedure outlined in [4],

relationship between crack tip stresses and far-field stresses can be found:

$$R\sigma_t = \left[1+\frac{3(3+\nu)(1-\nu)\gamma}{2\Gamma}\alpha_{bb}\right]\sigma_q - \frac{1-\nu^2}{2}\frac{\gamma}{\Gamma}\alpha_{tb}m_p \tag{9}$$

$$R\sigma_b = -\frac{3(3+\nu)(1-\nu)}{2}\frac{\gamma}{\Gamma}\alpha_{bt}\sigma_q + \left[1+\frac{1-\nu^2}{2}\frac{\gamma}{\Gamma}\alpha_{tt}\right]m_p \tag{10}$$

$$T\tau_t = \left[1+\frac{3(1+\nu)}{2}\frac{\gamma}{\Gamma}C_{bb}\right]\sigma_{pq} - \frac{1+\nu}{2}\frac{\gamma}{\Gamma}C_{tb}m_{pq} \tag{11}$$

$$T\tau_b = -\frac{3(1+\nu)}{2}\frac{\gamma}{\Gamma}C_{bt}\sigma_{pq} + \left[1+\frac{1+\nu}{2}\frac{\gamma}{\Gamma}C_{tt}\right]m_{pq} \tag{12}$$

Where

$$R = \left[1+\frac{1-\nu^2}{2}\frac{\gamma}{\Gamma}\alpha_{tt}\right]\left[1+\frac{3(3+\nu)(1-\nu)\gamma}{2\Gamma}\alpha_{bb}\right] - \frac{3(1-\nu)(3+\nu)(1-\nu^2)}{4}\left(\frac{\gamma}{\Gamma}\right)^2{\alpha_{bt}}^2$$

and

$$T = \left[1+\frac{3(1+\nu)\gamma}{2\Gamma}C_{bb}\right]\left[1+\frac{1+\nu}{2}\frac{\gamma}{\Gamma}C_{tt}\right] - \frac{3(1+\nu)^2}{4}\left(\frac{\gamma}{\Gamma}\right)^2{C_{tb}}^2$$

In above relations, $\alpha_{ij}, i, j = t, b$, $\alpha_{bt} = \alpha_{tb}$ are compliance coefficients used to match stretching and bending resistances in mode **I** which happens in symmetric loading case. $C_{ij}, i, j = b, t$, $C_{bt} = C_{tb}$ are coefficients for handle anti-symmetric and mixed mode loading where modes **II** and **III** of crack are excited[2]. Expressions which are used to evaluate these quantities according to crack depth ratio (ζ) are given in Appendix A.

By using transforming equations (3-4) and relations (9-12) closure forces and moments of crack will be in hand. More detail calculations are given in Appendix B for the sake of convenience.

From Kirchhoff hypothesis, bending moments M_{xx}, M_{yy}, M_{xy} are given in dimensionless coordinates as follows:

$$M_{xx} = \frac{D}{l_1^2}\left(\frac{\partial^2 w}{\partial\xi^2}+\frac{\nu}{\phi^2}\frac{\partial^2 w}{\partial\eta^2}\right) \tag{13}$$

$$M_{yy} = -\frac{D}{l_1^2}\left(\frac{\partial^2 w}{\partial\eta^2}+\nu\phi^2\frac{\partial^2 w}{\partial\xi^2}\right) \tag{14}$$

$$M_{xy} = M_{yx} = -\frac{D(1-\nu)\phi}{l_1^2}\left(\frac{\partial^2 w}{\partial\xi\partial\eta}\right) \tag{15}$$

Using equations 13-15 and ones given in Appendix B which present crack closure forces and moments, final partial differential equation that governs dynamics of part-through cracked plate will be in hand:

$$\begin{aligned}
&(1-\Lambda_{11})\frac{\partial^4 w}{\partial\eta^4}+\phi^2(2-\Lambda_{12})\frac{\partial^4 w}{\partial\xi^2\partial\eta^2}+\\
&\phi^4(1-\Lambda_{10})\frac{\partial^4 w}{\partial\xi^4}+\frac{\rho h\phi^4 l_1^4}{D}\frac{\partial^2 w}{\partial t^2}=\\
&\frac{\phi^4 l_1^4}{D}F\delta(\xi-\xi_0)\delta(\eta-\eta_0)\\
&+N_x\frac{\phi^2 l_1^2}{D}\left[\Lambda_1\frac{\partial^2 w}{\partial\xi^2}+\Lambda_2\frac{\partial^2 w}{\partial\eta^2}+2\Lambda_3\frac{\partial^2 w}{\partial\xi\partial\eta}\right]+\\
&\phi^3\Lambda_{22}\frac{\partial^4 w}{\partial\xi^3\partial\eta}+\phi\Lambda_{23}\frac{\partial^4 w}{\partial\eta^3\partial\xi}\\
&+N_y\frac{\phi^2 l_1^2}{D}\left[\Lambda_4\frac{\partial^2 w}{\partial\eta^2}+\Lambda_5\frac{\partial^2 w}{\partial\xi^2}+2\Lambda_6\frac{\partial^2 w}{\partial\xi\partial\eta}\right]+\\
&N_{xy}\frac{\phi^2 l_1^2}{D}\left[2\Lambda_7\frac{\partial^2 w}{\partial\xi\partial\eta}+\Lambda_8\frac{\partial^2 w}{\partial\xi^2}+\Lambda_9\frac{\partial^2 w}{\partial\eta^2}\right]\\
&-\phi(1-\nu)\left[\Lambda_{19}\frac{\partial^2 w}{\partial\xi^2}+\Lambda_{20}\frac{\partial^2 w}{\partial\eta^2}+2\Lambda_{21}\frac{\partial^2 w}{\partial\xi\partial\eta}\right]\frac{\partial^2 w}{\partial\xi\partial\eta}-\\
&\left[\phi^2\frac{\partial^2 w}{\partial\xi^2}+\nu\frac{\partial^2 w}{\partial\eta^2}\right]\left[\Lambda_{13}\frac{\partial^2 w}{\partial\xi^2}+\Lambda_{14}\frac{\partial^2 w}{\partial\eta^2}+2\Lambda_{15}\frac{\partial^2 w}{\partial\xi\partial\eta}\right]\\
&-\left[\phi^2\nu\frac{\partial^2 w}{\partial\xi^2}+\frac{\partial^2 w}{\partial\eta^2}\right]\left[\Lambda_{16}\frac{\partial^2 w}{\partial\xi^2}+\Lambda_{17}\frac{\partial^2 w}{\partial\eta^2}+2\Lambda_{18}\frac{\partial^2 w}{\partial\xi\partial\eta}\right]
\end{aligned} \tag{16}$$

Where $\Lambda_1 - \Lambda_{23}$ are provided in Appendix C. In Equation (16), in-plane membrane forces (N_x, N_y and N_{xy}) can be rewritten using Berger's formulation[8] to reach to an explicit equation in which the transverse displacement of plate (*w*) is the only dependent variable*:*

$$\begin{aligned}
N_x &= \frac{6D}{\gamma^2 l_1^4}\int_0^1\int_0^1\left[\left(\frac{\partial w}{\partial\xi}\right)^2+\frac{\nu}{\phi^2}\left(\frac{\partial w}{\partial\eta}\right)^2\right]d\xi d\eta\\
N_y &= \frac{6D}{\gamma^2 l_1^4}\int_0^1\int_0^1\left[\nu\left(\frac{\partial w}{\partial\xi}\right)^2+\frac{1}{\phi^2}\left(\frac{\partial w}{\partial\eta}\right)^2\right]d\xi d\eta\\
N_{xy} &= \frac{12D(1-\nu)}{\gamma^2 l_1^4\phi}\int_0^1\int_0^1\left[\left(\frac{\partial w}{\partial\xi}\frac{\partial w}{\partial\eta}\right)\right]d\xi d\eta
\end{aligned} \tag{17}$$

2.1. Time domain solution

By Eq. 16 being in hand, approximate solution of the nonlinear PDE would be possible by application of Galerkin method. In this research, time domain type of solution is required and therefore convergence study about the minimum number of mode-shapes is imperative to reach acceptable accuracy. According to various boundary conditions of the plate, different mode-shape functions are considered as follows:

For fully simply-supported plate (SSSS):

$$w(\xi,\eta) = \sum_{i=1}^{\infty}\sum_{j=1}^{\infty}\sin(i\pi\xi)\sin(j\pi\eta)\varphi_{ij}(t) \tag{18}$$

two opposite sides are clamped while remaining edges are simply supported: (SSCC)

$$\begin{aligned}\dot{\tilde{x}} &= \varepsilon(10(\tilde{y}-\tilde{x})),\\ \dot{\tilde{y}} &= \varepsilon((28-\tilde{z})-\tilde{y}),\\ \dot{\tilde{z}} &= \varepsilon(\tilde{x}\tilde{y}-\frac{8}{3}\tilde{z}).\end{aligned} \tag{21}$$

$$w(\xi,\eta)=\sum_{i=1}^{\infty}\sum_{j=1}^{\infty}\begin{pmatrix}-\cos(co_i\xi)+\cosh(co_i\xi)\\ +\dfrac{\cos(co_i)-\cosh(co_i)}{\sinh(co_i)-\sin(co_i)}\\ \left[\sinh(co_i\xi)-\sin(co_i\xi)\right]\end{pmatrix}\sin(j\pi\eta)\varphi_{ij}(t) \tag{19}$$

And if all of the edges are fully restrained (CCCC):

$$\begin{aligned}w(\xi,\eta)=&\sum_{i=1}^{\infty}\sum_{j=1}^{\infty}\begin{pmatrix}-\cos(co_i\xi)+\cosh(co_i\xi)\\ +\dfrac{\cos(co_i)-\cosh(co_i)}{\sinh(co_i)-\sin(co_i)}\\ \left[\sinh(co_i\xi)-\sin(co_i\xi)\right]\end{pmatrix}\\ &\times\begin{pmatrix}-\cos(co_j\eta)+\cosh(co_j\eta)+\\ \dfrac{\cos(co_j)-\cosh(co_j)}{\sinh(co_j)-\sin(co_j)}\\ \left[\sinh(co_j\eta)-\sin(co_j\eta)\right]\end{pmatrix}\varphi_{ij}(t)\end{aligned} \tag{20}$$

Where $co_{i,j}$ are coefficients given in Appendix D and $\varphi_{ij}(t)$s are temporal functions which determine the evolutions of the system's dynamic in time domain. Above infinite series must be truncated in practical applications and the number of modes must be selected in such a way that acceptable accuracy is achievable for subsequent time series analysis. Considering desired boundary condition and by substitution of one of the relations (18-20) into equation (16) and application of Galerkin's residual weight procedure, a system of coupled nonlinear temporal differential equations would be obtained.

2.2. Convergence Study and Comparison with FE Model

In this section for evaluation of feasibility of the implemented method and also study of convergence of established nonlinear model a detailed FE model of part-through cracked plate is developed in Abaqus/Explicit environment. Mentioned model due to thin wall structure of the plate and also partially penetrating crack configuration is essentially a three-dimensional problem and hence requires considerable number of three dimensional elements. Therefore, a plate with dimensions $l_1\times l_2\times h=1\times1\times0.02$ m which contains a crack with depth ratio of $\zeta=0.7$ and length parameter of $\Gamma=0.15$ is considered $\nu=0.33,\ \rho=2660(kg/m^3)$. It is assumed that crack shape is rectangular and plane of discontinuity is perpendicular to the plane of the plate. Material properties of plate are set as follows: E=70e9 GPa, . It is assumed that a mass proportional damping mechanism equal to one percent of critical damping is existed for both of FE and analytical models (i.e. μ must be set for every vibration mode to assign 1 % of critical linear viscous damping, accordingly). Moreover, for sake of simplicity in meshing of the model, crack was set to be parallel to x-direction and is located in center of the plate. Figure 3 shows schematic of the proposed problem and its numerical equivalence in FE software. There are162905 elements that are used to construct the numerical model. Seam feature is implemented to assign a geometric discontinuity into the model. Chaotic signal is itself a broad bandwidth one and due to the forced vibration essence of present problem, using of this type of signal is feasible for examining the analytical model and the convergence study. For excitation of the models a chaotic Lorenz type system of equations is considered which is given as follows[23] :

where over-dot operator denotes the derivation respect to time and $\tilde{x}, \tilde{y}$ and $\tilde{z}$ are Lorenz's equation variables from which only $\tilde{x}$ will be used to make amplitude of excitation force (i.e. $\boldsymbol{F}$ in equation (16)). ε is tuning parameter which will be discussed in more detail in next section. However, in this stage, $\varepsilon=3$ is used for comparison between FE model and nonlinear analytical models of SSSS-SSCC and $\varepsilon=4$ for CCCC boundary condition. It must be noted that raw exciting amplitude (i.e. $\tilde{x}$) extracted directly from Lorenz model may not be sufficient to produce desired transverse deflection (w) in real model, thus a magnification factor must be multiplied to $\tilde{x}$ to achieve a deflection in order of the thickness of the plate.

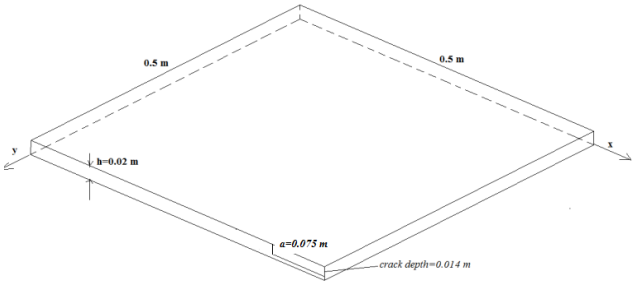

(a)

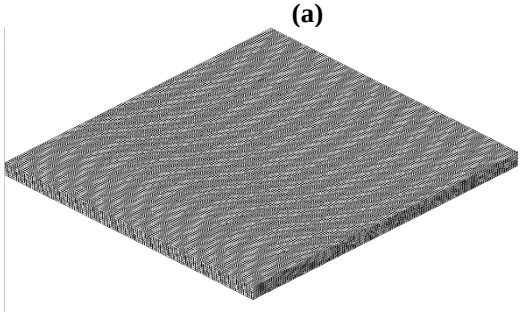

(b)

Figure 3. (a) Schematic configuration of cracked plate for convergence and verification study, only one quarter of plate depicted to better caption of crack, (b) three dimensional FE model.

The exciting force is applied in $x_0=y_0=0.4$m. Figure 4 summarizes the results of detailed numerical simulations and its comparison with analytical model for various boundary conditions. Adams-Gear algorithm was used for numerical integration of system of nonlinear ODEs. Neglecting transient part of solutions in which a slight departing of results is

perceptible, a good correlation between analytical model and detailed numerical simulations is observed in steady state response. This does not produce notable circumstances due to omitting of transient parts of solutions in attractor analysis, hence it can be implied that proposed model has sufficient eligibility for subsequent analysis in time series domain.

3. Tuned Chaotic Interrogation

As mentioned in the previous researches[16][15][19], chaotic signal due to its characteristics, such as wide frequency spectrum, determinism and sensitivity to the initial conditions may be a noble signal to be exploited as an interrogation tool to find evidences of malfunctions in dynamical systems. In fact, presence of positive Lyapunov exponents in spectrum of chaotic systems can lead to extreme sensitivity to the small changes of the interrogated system's parameters. Although aforementioned method of interrogation has its advantages, some subtleties arise due to the tuning procedures. Introducing damage to the dynamical system results in change of its eigen-structure. If Lyapunov exponent spectrum (LEs) of the system and chaotic signal are overlapped, then this ensures that changes in LEs of structure due to damage (e.g. crack) will have effect on the Lyapunov dimension of the filtered chaotic signal [16]which is defined according to the Kaplan-Yorke conjecture[24] as:

$$D_L = K + \frac{\sum_{m=1}^{K} \lambda_m}{-\lambda_{K+1}} \tag{22}$$

In which, K is the number of exponents that may be added before the sum becomes negative and λ_m is the Lyapunov exponents.

(a)

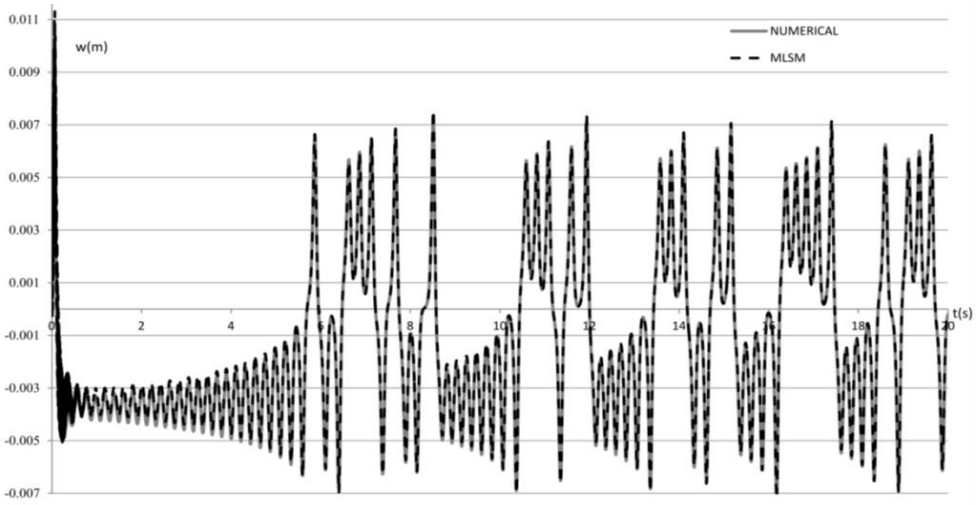

(b)

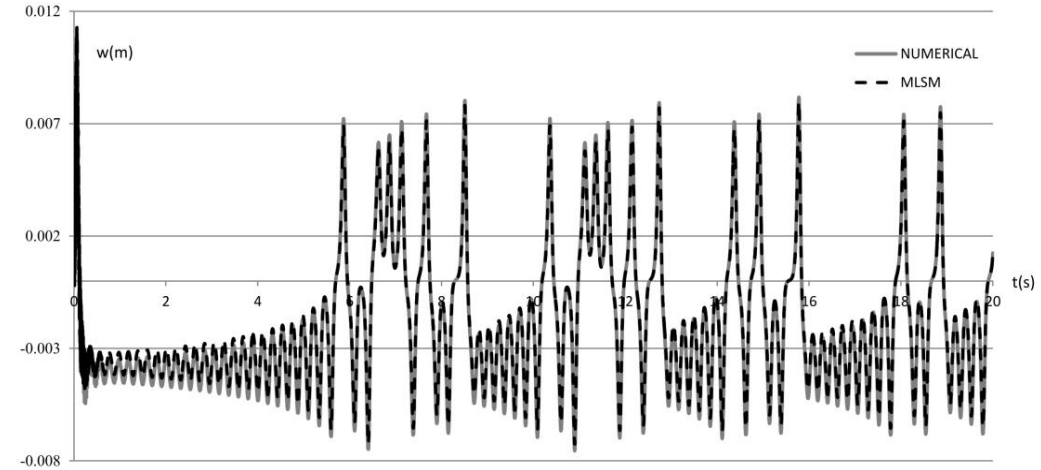

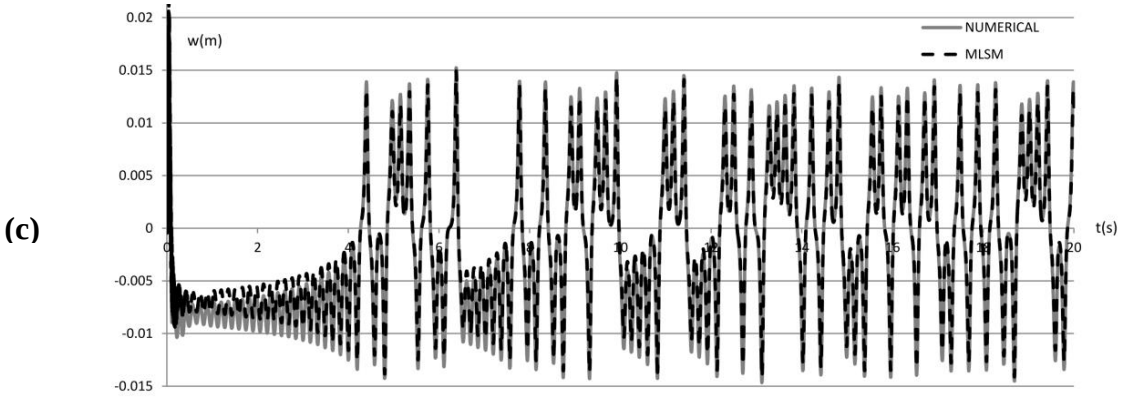

Figure 4. Convergence study of MLSM nonlinear model and comparison with detail FE model, time history of deflection at center of the plate; (a)SSSS B.C. $F=100*\tilde{x}$: 4 dof, $\varphi_{1,1},\varphi_{1,3},\varphi_{3,1},\varphi_{3,3}$ (b)SSCC B.C. $F=200*\tilde{x}$: 9dof, $\varphi_{1,1},\varphi_{1,3},\varphi_{3,1},\varphi_{3,3},\varphi_{1,5},\varphi_{5,1},\varphi_{3,5},\varphi_{5,3},\varphi_{5,5}$ (c): CCCC B.C. $F=600*\tilde{x}$:12dof, $\varphi_{1,1},\varphi_{1,3},\varphi_{3,1},\varphi_{3,3},\varphi_{1,5},\varphi_{5,1},\varphi_{3,5},\varphi_{5,3},\varphi_{5,5},\varphi_{3,7},\varphi_{7,3},\varphi_{7,7}$

3.1. Nonlinear Prediction Error as a Feature

One of the most important aspects of structural health monitoring is the selection of an appropriate feature which has an acceptable level of sensitivity to damage parameters' alteration. State-space response of dynamical systems has essentially a geometrical configuration. Chaotic attractor of an exciting signal after passing from filter of a degraded structure's model (i.e. cracked plate), encounters an alteration in its primary geometrical topology. The nonlinear prediction error (**NPE**) is one metric that describes the ability of prediction of state of a system in future by an attractor. This approach was originally established to investigate the non-stationarity of time-series[25]. If this metric examines the prediction ability of two attractors which are constructed from time-series recorded in various conditions of structure (e.g. various crack lengths, orientation etc.) but from a fixed measuring point, then it is called auto-prediction error. Alongside of this definition, if comparison is taken place between two different attractors which are recorded from different measurement points and disparate conditions then concept of cross-prediction error can be defined. [19]. In this article nonlinear auto-prediction error (**NAPE**) will be used as a damage sensitive feature.

For quantifying mentioned feature, an attractor which is constructed from a reference condition of structure (i.e. an intact plate) is considered as a baseline attractor. Attractors which are constructed from subsequent conditions of plate as it is degraded are called comparison attractors. Some points called fiducial points are randomly selected on the comparison attractor and according to geometrical coordinates of these fiducial points another set of points in neighborhood of those coordinates are found on the baseline attractor. Fiducial points on the comparison attractor and also corresponding neighborhood points on the baseline attractor are evolved in time by a few steps. New position of evolved points can be used to determine the Euclidean centroid of neighborhood points on the baseline attractor and can be compared with the time evolved fiducial coordinates on the comparison attractor. The Euclidean distance between centroid of time evolved neighborhood points and corresponding time

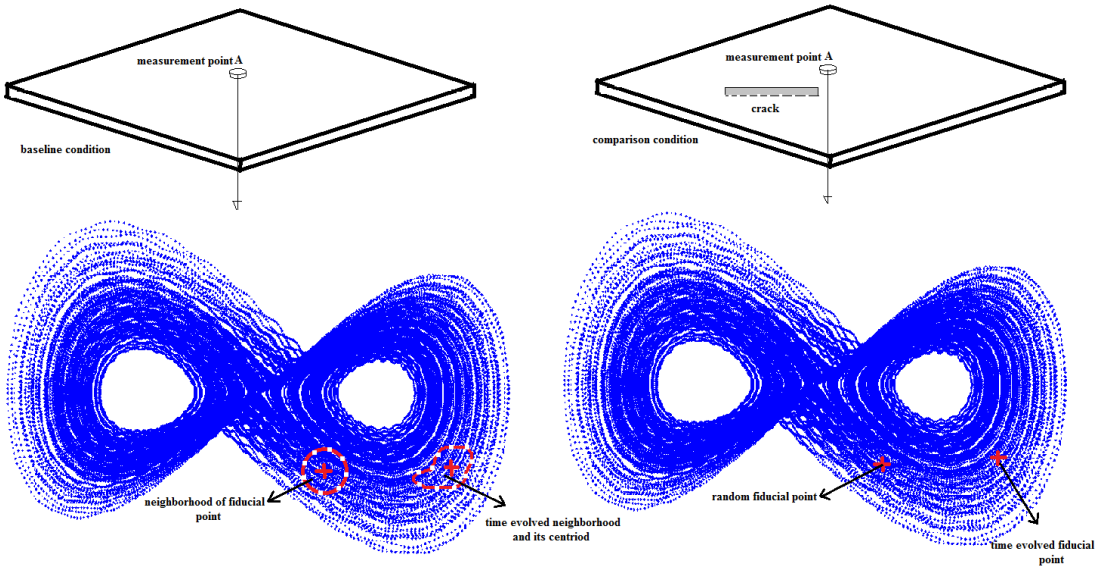

Figure 5. Qualitative illustration of Nonlinear Auto-prediction Error (NAPE) calculation algorithm

evolved fiducial point can be evaluated as a metric which is called **NAPE,** e_1. Number of randomly selected points on the comparison attractor is depended on the numbers of points which are used to construct attractor[19]. Finally, an averaging must be carried out on all of the Euclidean distances (corresponding to every fiducial point) calculated in preceding stage to obtain an estimation of NAPE. Further mathematical description of NAPE can be found in [19]. Figure 5 illustratively describes the above-mentioned algorithm for calculation of **NAPE.**

In most of applications normalized form of this quantity is used. Here, this normalization is carried out by definition of:

$$e = \frac{e_1 - e^*}{e^*} \tag{23}$$

Where, e is normalized NAPE, e_1 is the quantity which was calculated according to above outlined algorithm and e^* is the quantity of un-normalized NAPE when two compared attractors are identical and are set to be the baseline attractor, i.e. attractor corresponding to the intact plate.

3.2. Lyapunov Exponents Spectrums Crossing

In this article, Lyapunov spectrum of the nonlinear model of plate with the properties are specified in section 2.3 and chaotic signal are calculated numerically according to an algorithm outlined in [26] for a base condition of the structure which here is assumed to be the intact plate. For calculation of Lyapunov exponents it is assumed that one percent of mass proportional damping mechanism is existed in the plate. If tuning parameter in chaotic signal is set to be $\varepsilon = 1$, then LEs of exciting signal will be ($\approx 0.82, 0, -14.5$). By controlling LEs of the intact plate ((see Figure 6), condition of overlapping of spectrums for all of boundary condition cases is met. This guarantees that any changes in eigen structure of the cracked plate model results in an alteration of Lyapunov dimension of filter-passed chaotic signal. While, the required condition of signal tuning is met this process may be further scrutinized by checking the effect of variation of tuning parameter on the sensitivity of NAPE.

3.3. Effect of Tuning Parameter on Feature Sensitivity

As it can be concluded that by crossing of LEs spectrums of signal with the structural model a change in Lyapunov dimension of exciting signal is guaranteed but this alteration may not lead to an acceptable level of sensitivity. By changing the tuning parameter within a range and calculation of NAPE feature for two states of damage limits e.g. maximum crack length ($\Gamma = 0.25$) and intact condition, variation of feature vs. tuning parameter can be evaluated. It is assumed that crack orientation is parallel to x-axis and its depth parameter is fixed to be $\zeta = 0.7$ for these calculations. Figure 6 illustrates the behavior of NAPE vs. tuning parameter, ε. What is more discernible from these graphs is the existence of a distinct span in which the normalized NAPE (***e***) takes higher magnitudes. For SSSS and SSCC boundary conditions apex of the curve is located around $\varepsilon = 3.5$ and this maximum migrates to vicinity of $\varepsilon = 5$ in CCCC case. Also, there is a considerable reduction in value of ***e*** in fully clamped case. Studies in subsequent sections are accomplished by setting $\varepsilon = 3.5$ for SSSS and SSCC and $\varepsilon = 5$ for CCCC boundary conditions. Figure 7 summarizes the graphical depiction of final LEs spectrums of intact plate model and tuned signal for different boundary conditions.

4. Results and Discussion

In this section the results of analyses are presented after the tuned chaotic interrogator signal used to excite a cracked plate with $\phi = \frac{l_1}{l_2} = \frac{1(m)}{1(m)} = 1$ and h=0.02(m) as its geometrical characteristics. Material of the plate is assumed to be linear isotropic elastic with properties provided in the section 2.2.

Alteration in geometrical configuration of chaotic attractor after passing from filter of cracked plate with various levels of damage intensity (e.g. crack length) is illustrated in figure 8. This figure depicts the local morphing of attractors as a result of damage action on the nonlinear model.

Figure 9 illustrates variation of normalized NAPE (e) vs. variation of crack length parameter, Γ For various boundary conditions. For these analyses crack depth parameter is assumed to be constant, $\zeta = 0.7$. Crack orientation for SSSS and CCCC cases is varied in range of $0^o \le \theta \le 45^o$ in 15º intervals due to symmetry and in the case of SSCC this range extended to $0^o \le \theta \le 90^o$ with 30º intervals.

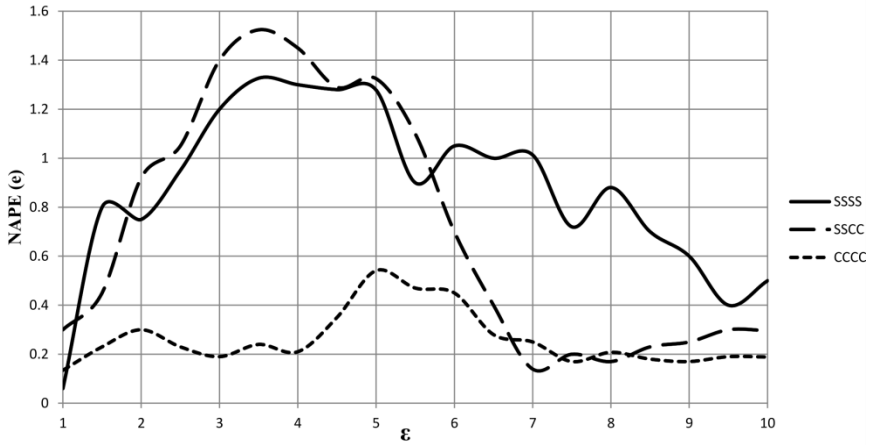

Figure 6. NAPE vs. tuning parameter(ε)

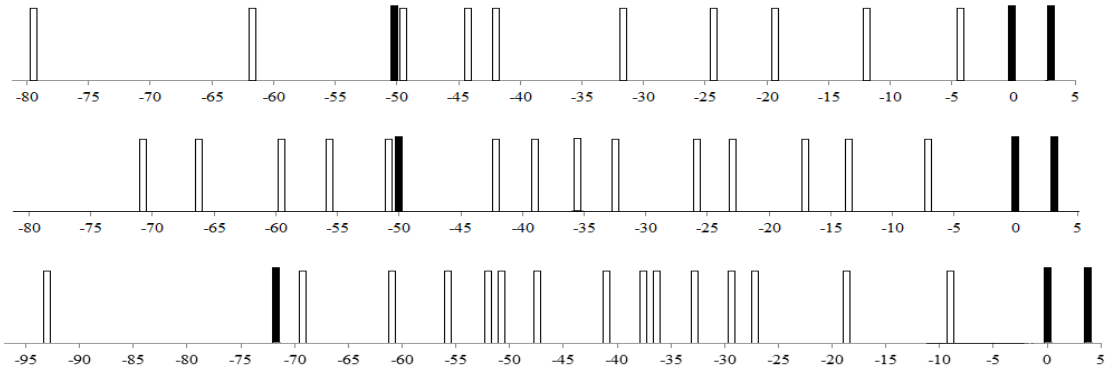

Figure 7. Crossing Lypunov Exponents Spectrums (LEs) of the intact plate model (by assuming 0.01 (one percent) of mass proportional damping) and chaotic signal after optimal tuning for top: SSSS, middle: SSCC and bottom: CCCC boundary conditions (Whit bars: model, Black bars: Chaotic signal).

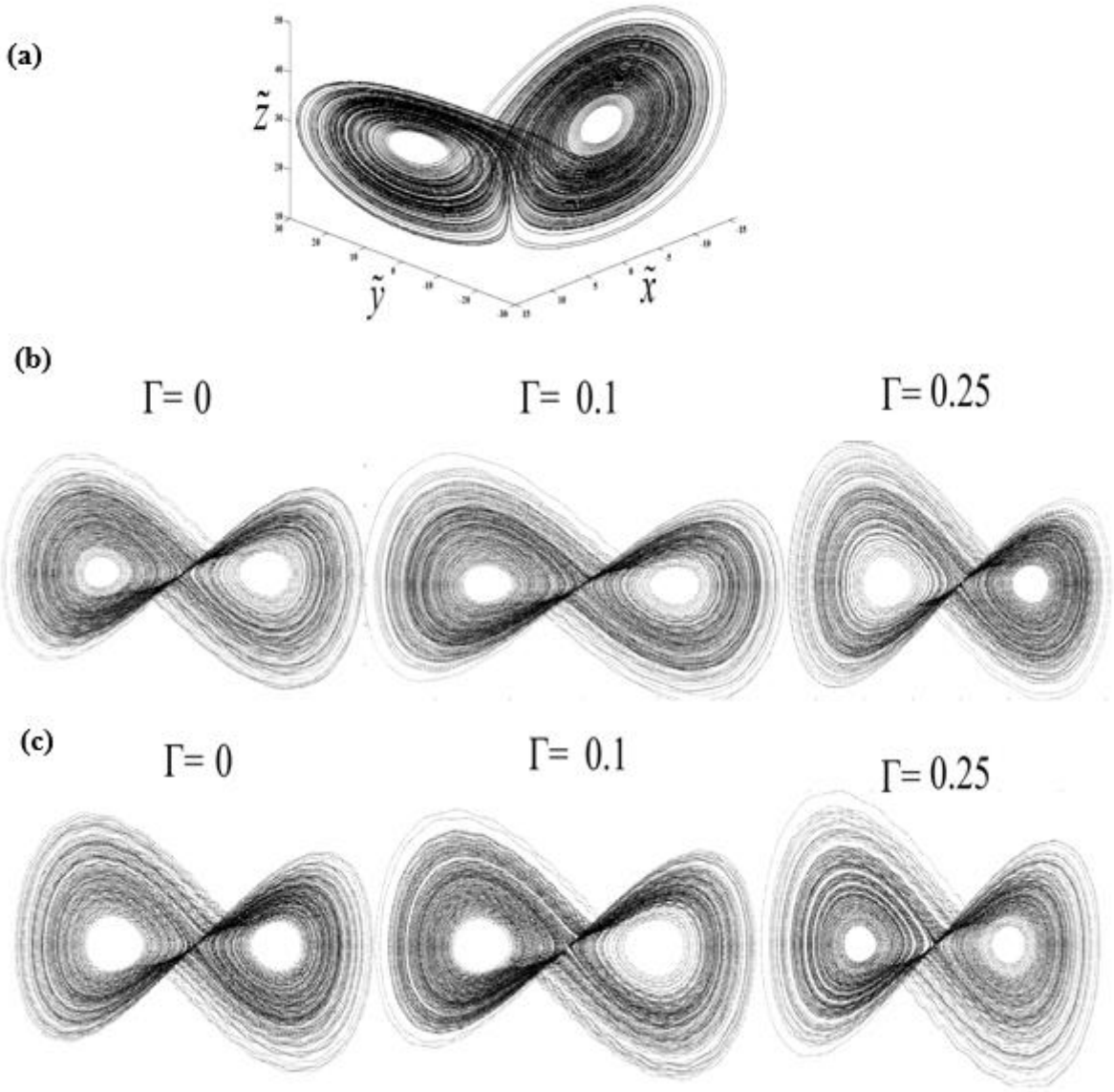

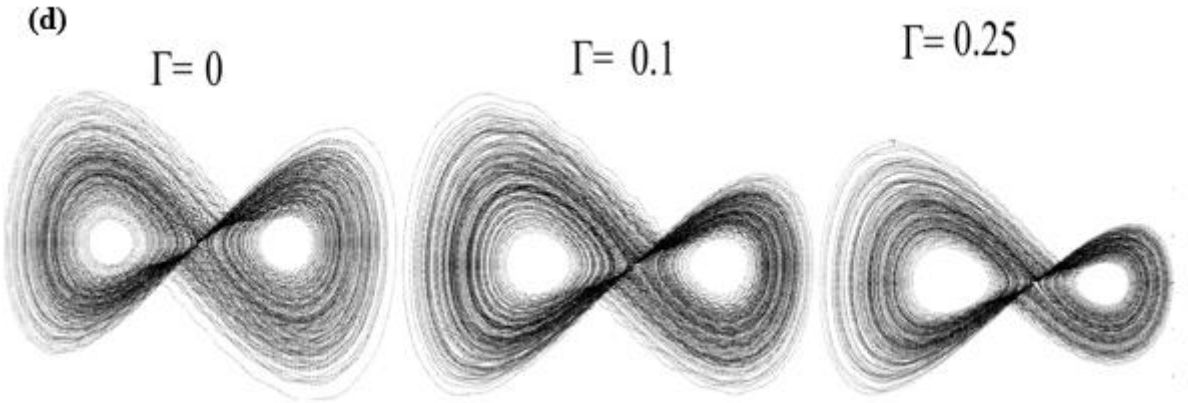

Figure 8. Chaotic attractor morphing after passing from filter of the model for different damage intensities, a) Lorenz chaotic signal, b) SSSS, c)SSCC and d) CCCC boundary condition. State space at center of centrally cracked plate when crack is parallel to x axis.

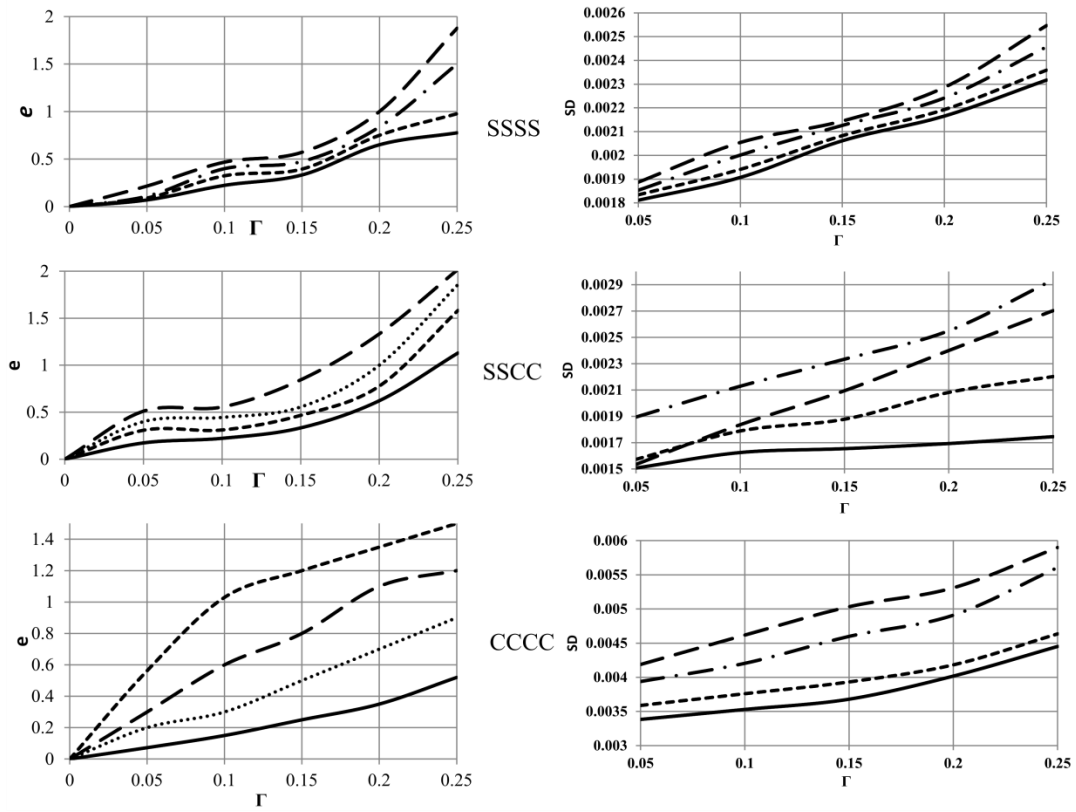

Figure 9. Variation of NAPE (left) and Standard Deviation (right) vs. crack length parameter (Γ) for various boundary conditions and crack orientations, legend for SSCC :0° ——— , 30° - - - ,60° —·— ,90° — — , SSSS and CCCC: 0° ——— , 15° - - - ,30° —·— ,45° — — .

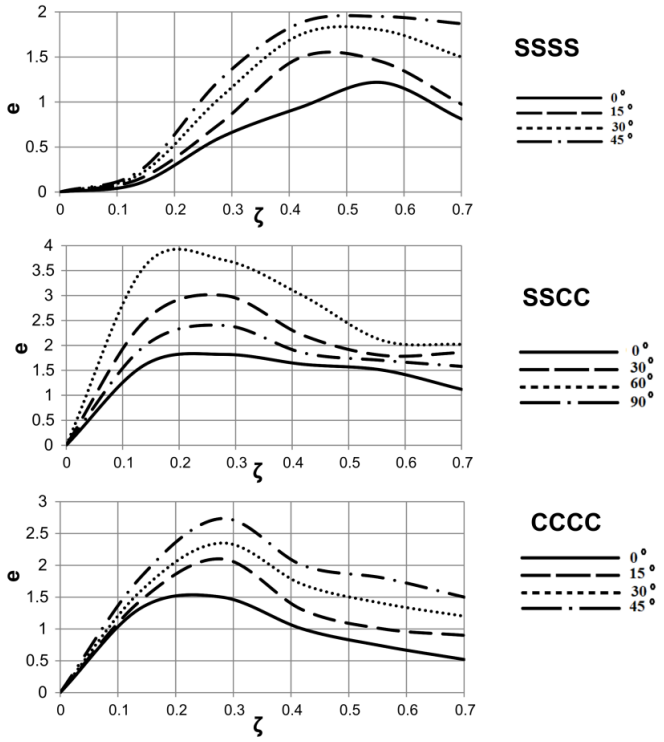

Figure10. Variation of normalized NAPE (e) versus crack depth parameter (ζ)

For SSSS case, maximum normalized NAPE factor (***e***) can take the excellent value of 1.85 (i.e. 185%) where the crack is centrally located and inclined by 45° angle. Maximum sensitivity of ***e*** corresponding to $\Gamma = 0.05$ as shortest crack length is about 24%. This graph reveals this fact that distinguishing between various crack orientations is a relatively hard task for SSSS boundary condition at least in real world experimental conditions.

In SSCC case, maximum excellent value of 2 (200%) for ***e*** is attained in centrally cracked plate corresponding to $\Gamma = 0.25$. Maximum achievable value of ***e*** corresponding to $\Gamma = 0.05$ is about 50% and occurred in crack orientation of to 60°.

Maximum quantity of 1.5 for ***e*** is observable in center located crack case for fully clamped (CCCC) boundary condition. Generally lower sensitivity for this case is elicitable in comparison with other boundary conditions. 60% of sensitivity for $\Gamma = 0.05$ and 45° of crack angle is observed which is higher than sensitivity for similar conditions in SSSS case.

By comparing the various boundary conditions, what is more discernible is that by more restraining the plate distinguishing of various crack orientations would be easier task. It is noteworthy that in the case of presence of multiple cracks in the plate which is more probable in real conditions, it is expectable that the only NPE is not sufficient for high levels of health monitoring. In this case, it is suggested that the number of features and also the measurement locations in various points of the plate must be increased. For example, the standard deviation of the time series could be a good candidate to be a bonus damage sensitive feature. Standard deviation is defined as:

$$SD = \sqrt{\frac{\sum_{r=1}^{N}\left(x_r - \bar{x}\right)^2}{N-1}} \tag{23}$$

where x_r, $r = 1,...,N$, denotes to individual data points resulted from time series solution, $\bar{x}$ is the mean of data set and *N* is the number of time series data set. Figure 9 illustrates the variation of standard deviation vs. crack length parameter which shows a considerable sensitivity to the damage severity. By gathering more information from multiple points of the plate, judgment about the severity and location of cracks may be facilitated.

Figure 10 presents effect of crack depth parameter, ζ , on the variation of ***e***. It is assumed that the crack is located in center of the plate. What is more discernible from these graphs is non-monotonic behavior of ***e*** against ζ . There is an extremum for every boundary condition that its location depends on the crack angle. While maximum quantity of ***e*** for SSSS case is observed for higher values of ζ ($\approx 0.4-0.5$), these points located in range of $0.2 \le \zeta \le 0.3$ for SSCC and CCCC boundary conditions.

Table 1 summarizes the variation of natural frequencies of cracked plate for various boundary conditions at most sensitive crack orientations. This table illustrates the sensitivity level of conventional frequency based method and indicates the superiority of chaotic excitation method.

Table 1. Comparison of fundamental frequency for various crack lengths

B.C.	(crack orientation) θ°	First Natural Frequency(Hz) for Γ=0.05	First Natural Frequency(Hz) for Γ=0.25	% of sensitivity
SSSS	0°	93.5	81.01	13%
SSCC	90°	133	113	15%
CCCC	45°	155	138	11%

5. Conclusion

In present article, nonlinear time series response of a rectangular partially through cracked plate subjected to the chaotic excitation studied in state space domain. For more comprehensive investigation of the crack effect on the variation of damage sensitive feature an analytical model developed using MLSM theory, which its eligibility for time series analysis examined through the comparison with a detailed FE model. By implementation of a tuned Lorenz type chaotic signal to excite the cracked plate which constrained with different boundary conditions, sensitivity of nonlinear auto-prediction error (NAPE) as a feature is examined. Crack characteristics such as depth, length, orientation and location are selected as damage parameters. Scrutinizing the results showed that variation of the proposed attractor based feature versus damage parameters is significant due to high sensitivity of NAPE to local morphing of the filter-passed chaotic attractor.

By deviation of crack location from center of the plate, an asymptotic behavior for NAPE (e) is observable in SSSS and SSCC cases while this behavior is negligible for fully clamped case. Although there is a monotonic relation between NAPE and crack length parameter such a behavior is not observable in the case of crack depth factor. In addition, NAPE discrimination level for various crack angles is noticeable. High capability of chaotic interrogation and geometrical evaluation of attractors in damage assessment of thin walled cracked structures can be implied from mentioned properties. Although present purely theoretical study illustrated the high sensitivity of proposed method to various damage variations, however in practical applications effect of noise can cause to mitigation of sensitivity and this problem may be studied in a separate experimental program.

References

[1] J. R. Rice and N. Levy, "The part-through surface crack in an elastic plate," *Journal of applied mechanics,* vol. 39, no. 1, pp. 185-194, 1972.

[2] P. Joseph and F. Erdogan, "Surface crack in a plate under antisymmetric loading conditions," *International Journal of Solids and Structures,* vol. 27, no. 6, pp. 725-750, 1991.

[3] Y. S. Wen and Z. Jin, "On the equivalent relation of the line spring model: A suggested modification," *Engineering Fracture Mechanics,* vol. 26, no. 1, pp. 75-82, 1987.

[4] Z. Zhao-Jing and D. Shu-Ho, "Stress intensity factors for an inclined surface crack under biaxial stress state," *Engineering fracture mechanics,* vol. 47, no. 2, pp. 281-289, 1994.

[5] F. Delale, "Cracked shells under skew-symmetric loading," *International Journal of Engineering Science,* vol. 20, no. 12, pp. 1325-1347, 1982.

[6] Z.-Q. Cheng and J. Reddy, "Green's functions for an anisotropic thin plate with a crack or an anticrack," *International journal of engineering science,* vol. 42, no. 3, pp. 271-289, 2004.

[7] A. Israr, M. P. Cartmell, E. Manoach, I. Trendafilova, M. Krawczuk, and Ł. Arkadiusz, "Analytical modeling and vibration analysis of partially cracked rectangular plates with different boundary conditions and loading," *Journal of Applied Mechanics,* vol. 76, no. 1, p. 011005, 2009.

[8] H. M. Berger, "A new approach to the analysis of large deflections of plates," 1954.

[9] R. Ismail and M. Cartmell, "An investigation into the vibration analysis of a plate with a surface crack of variable angular orientation," *Journal of Sound and Vibration,* vol. 331, no. 12, pp. 2929-2948, 2012.

[10] T. Bose and A. Mohanty, "Vibration analysis of a rectangular thin isotropic plate with a part-through surface crack of arbitrary orientation and position," *Journal of Sound and Vibration,* vol. 332, no. 26, pp. 7123-7141, 2013.

[11] T. Li, X. Zhu, Y. Zhao, and X. Hu, "The wave propagation and vibrational energy flow characteristics of a plate with a part-through surface crack," *International Journal of Engineering Science,* vol. 47, no. 10, pp. 1025-1037, 2009.

[12] T. Kuroiwa and H. Iemura, "Vibration-based damage detection using time series analysis," in *The 14th World Conference on Earthquake Engineering,* 2008, pp. 12-17.

[13] I. Trendafilova and E. Manoach, "Vibration-based damage detection in plates by using time series analysis," *Mechanical Systems and Signal Processing,* vol. 22, no. 5, pp. 1092-1106, 2008.

[14] E. Figueiredo, M. D. Todd, C. R. Farrar, and E. Flynn, "Autoregressive modeling with state-space embedding vectors for damage detection under operational variability," *International Journal of Engineering Science,* vol. 48, no. 10, pp. 822-834, 2010.

[15] J. Nichols, S. Trickey, M. Todd, and L. Virgin, "Structural health monitoring through chaotic interrogation," *Meccanica,* vol. 38, no. 2, pp. 239-250, 2003.

[16] J. Nichols, M. Todd, M. Seaver, and L. Virgin, "Use of chaotic excitation and attractor property analysis in structural health monitoring," *Physical Review E,* vol. 67, no. 1, p. 016209, 2003.

[17] J. Ryue and P. White, "The detection of cracks in beams using chaotic excitations," *Journal of sound and vibration,* vol. 307, no. 3, pp. 627-638, 2007.

[18] B. I. Epureanu, S.-H. Yin, and M. M. Derriso, "High-sensitivity damage detection based on enhanced nonlinear dynamics," *Smart Materials and Structures,* vol. 14, no. 2, p. 321, 2005.

[19] S. Torkamani, E. A. Butcher, M. D. Todd, and G. Park, "Hyperchaotic probe for damage identification using nonlinear prediction error," *Mechanical Systems and Signal Processing,* vol. 29, pp. 457-473, 2012.

[20] H. Makvandi, S. Moradi, D. Poorveis, and K. H. Shirazi, "A new approach for nonlinear vibration analysis of thin and moderately thick rectangular plates under inplane compressive load," *Journal of Computational Applied Mechanics,* 2017.

[21] R. Javidi, M. Moghimi Zand, and K. Dastani, "Dynamics of Nonlinear rectangular plates subjected to an orbiting mass based on shear deformation plate theory," *Journal of Computational Applied Mechanics,* 2017.

[22] M. Shishesaz, M. Kharazi, P. Hosseini and M. Hosseini, "Buckling Behavior of Composite Plates with a Pre-central Circular Delamination Defect under in-Plane Uniaxial Compression," *Journal of Computational Applied Mechanics,* vol. 48, no. 1, pp. 111-122, 2017.

[23] S. H. Strogatz, *Nonlinear dynamics and chaos: with applications to physics, biology, chemistry, and engineering*. Westview press, 2014.
[24] J. L. Kaplan and J. A. Yorke, "Chaotic behavior of multidimensional difference equations," in *Functional Differential equations and approximation of fixed points*: Springer, 1979, pp. 204-227.
[25] L. Y. Chang, K. A. Erickson, K. G. Lee, and M. D. Todd, "Structural Damage Detection using Chaotic Time Series Excitation," in *Proceedings of the 22st IMAC Conference on Structural Dynamics*, 2004.
[26] A. Wolf, J. B. Swift, H. L. Swinney, and J. A. Vastano, "Determining Lyapunov exponents from a time series," *Physica D: Nonlinear Phenomena*, vol. 16, no. 3, pp. 285-317, 1985.

Appendix A

According to calculations of Levy and Rise[1], α_{ij} compliance coefficients are varied as a function of ζ (crack depth ratio) :

$$\alpha_{tt}=\zeta^2(1.98-0.54\zeta+18.65\zeta^2-33.7\zeta^3+99.26\zeta^4-211.90\zeta^5+436.84\zeta^6-460.48\zeta^7+289.98\zeta^8) \quad \text{A.1}$$

$$\alpha_{tb}=\zeta^2(1.98-1.91\zeta+16.01\zeta^2-34.84\zeta^3+83.93\zeta^4-153.65\zeta^5+256.72\zeta^6-244.67\zeta^7+133.55\zeta^8) \quad \text{A.2}$$

$$\alpha_{bb}=\zeta^2(1.98-3.28\zeta+14.43\zeta^2-31.26\zeta^3+63.56\zeta^4-103.36\zeta^5+147.52\zeta^6-127.69\zeta^7+61.5\zeta^8) \quad \text{A.3}$$

Joseph and Erdoghan[2], derived compliance coefficients, C_{ij} for antisymmetric loading case as a function of crack depth ratio as follows:

$$C_{tt}=\int_0^{\zeta} f_1 f_1 d\zeta \quad \text{A.4}$$

$$C_{tb}=C_{bt}=\int_0^{\zeta} f_1 f_2 d\zeta \quad \text{A.5}$$

$$C_{bb}=\int_0^{\zeta} f_2 f_2 d\zeta \quad \text{A.6}$$

Where functions f_1, f_2 are defined as follows:

$$f_1(\zeta)=\sqrt{\frac{\zeta}{1-\zeta}}\begin{pmatrix}1-0.5\zeta+0.286163\zeta^2-0.2668\zeta^3+0.2215\zeta^4-0.1772\zeta^5+0.10906\zeta^6\\-0.044143\zeta^7+0.00806\zeta^8\end{pmatrix} \quad \text{A.7}$$

$$f_2(\zeta)=\sqrt{\frac{\zeta}{1-\zeta}}\begin{pmatrix}1-1.773776\zeta+0.9374\zeta^2-0.6028\zeta^3+1.176914\zeta^4-2.18323\zeta^5+\\2.90694\zeta^6-2.1219\zeta^7+0.659759\zeta^8\end{pmatrix} \quad \text{A.8}$$

Appendix B

By integration of transformation equations (3-4) and equations (9-12) over crack thickness, relation between closure forces and moments in p-q plane and far field forces and moments in x-y plane is funded as follow:

$$N_n=\Psi_1\left[N_x\sin^2\theta+N_y\cos^2\theta-N_{xy}\sin 2\theta\right]-\Psi_2\left[M_x\sin^2\theta+M_y\cos^2\theta\right] \quad \text{B.1}$$

$$M_n=-\Psi_3\left[N_x\sin^2\theta+N_y\cos^2\theta-N_{xy}\sin 2\theta\right]+\Psi_4\left[M_x\sin^2\theta+M_y\cos^2\theta\right] \quad \text{B.2}$$

$$N_t=\Psi_5\left[-\frac{N_x-N_y}{2}\sin 2\theta+N_{xy}\cos 2\theta\right]-\Psi_6\left[\frac{M_x-M_y}{2}\sin 2\theta\right] \quad \text{B.3}$$

$$M_t=-\Psi_7\left[-\frac{N_x-N_y}{2}\sin 2\theta+N_{xy}\cos 2\theta\right]+\Psi_8\left[\frac{M_x-M_y}{2}\sin 2\theta\right] \quad \text{B.4}$$

Where, Ψ_i, i=1-8 are listed as follows:

$$\Psi_1=\frac{1+\left(\frac{3(3+\nu)(1-\nu)\gamma}{2\Gamma}\alpha_{bb}\right)}{R};\qquad \Psi_2=\frac{3(1-\nu^2)}{R\Gamma l_1}\alpha_{tb};\qquad \Psi_3=\frac{(1-\nu)(3+\nu)\gamma^2 l_1}{4R\Gamma}\alpha_{tb}$$

$$\Psi_4=\frac{1+\frac{3(1-\nu^2)\gamma}{2\Gamma}\alpha_{tt}}{R};\qquad \Psi_5=\frac{1+\frac{3(1+\nu)\gamma}{2\Gamma}C_{bb}}{T};\qquad \Psi_6=\frac{3(1+\nu)\gamma}{2T\Gamma}C_{tb}$$

$$\Psi_7=\frac{(1+\nu)\gamma^2 l_1}{4T\Gamma}C_{bt};\qquad \Psi_8=\frac{1+\frac{(1+\nu)\gamma}{2\Gamma}C_{tt}}{T}$$

Where, ***R*** and ***T*** are defined in the text (see Eq. (12)).

Hence by using following expressions which act as reverse transformation from p-q to x-y plane:

$$\bar{N}_x = -(N_n \sin^2\theta - N_t \sin 2\theta)$$
$$\bar{N}_y = -(N_n \cos^2\theta + N_t \sin 2\theta) \qquad \text{B.6}$$
$$\bar{N}_{xy} = -(-N_n \frac{\sin 2\theta}{2} + N_t \cos 2\theta)$$
$$\bar{M}_x = -(M_n \sin^2\theta - M_t \sin 2\theta)$$
$$\bar{M}_y = -(M_n \cos^2\theta + M_t \sin 2\theta) \qquad \text{B.7}$$
$$\bar{M}_{xy} = -(-M_n \frac{\sin 2\theta}{2} + M_t \cos 2\theta)$$

Forces and moments due to presence of crack are written. Note that negative sign simulates reduction of forces and moments resulted from crack discontinuity [10],[9],[7].

Appendix C

Coefficients in equation (16), are listed as follows:

$$\Lambda_1 = 1 - \Psi_1 \sin^4(\theta) - \Psi_5 \frac{\sin^2 2\theta}{2}; \quad \Lambda_2 = -\Psi_1 \sin^2\theta \cos^2\theta + \Psi_5 \frac{\sin^2 2\theta}{2} \qquad \text{C.1, C.2}$$

$$\Lambda_3 = \left(\Psi_1 \sin^2\theta \frac{\sin 2\theta}{2} + \Psi_5 \frac{\sin 4\theta}{4} \right)\phi; \quad \Lambda_4 = 1 - \Psi_4 \cos^4\theta - \Psi_5 \frac{\sin^2 2\theta}{2} \qquad \text{C.3, C.4}$$

$$\Lambda_5 = \Lambda_2;\ \Lambda_6 = \left(\Psi_1 \cos^2\theta \frac{\sin^2 2\theta}{2} - \Psi_5 \frac{\sin 4\theta}{4} \right)\phi;\ \Lambda_7 = \left(1 - \Psi_1 \frac{\sin^2 2\theta}{2} - \Psi_5 \cos^2 2\theta \right)\phi \qquad \text{C.5, C.6, C.7}$$

$$\Lambda_8 = \Psi_1 \sin 2\theta \sin^2\theta + \Psi_5 \frac{\sin 4\theta}{2};\ \Lambda_9 = \Psi_1 \sin 2\theta \cos^2\theta - \Psi_5 \frac{\sin 4\theta}{2} \qquad \text{C.8, C.9}$$

$$\Lambda_{10} = \Psi_4 (\sin^2\theta + \nu \cos^2\theta) \sin^2\theta + \Psi_8 (1-\nu) \frac{\sin^2 2\theta}{2} \qquad \text{C.10}$$

$$\Lambda_{11} = \Psi_4 (\nu \sin^2\theta + \cos^2\theta) \cos^2\theta + \Psi_8 (1-\nu) \frac{\sin^2 2\theta}{2} \qquad \text{C.11}$$

$$\Lambda_{12} = \Psi_4 \left(\nu(\sin^4\theta + \cos^4\theta) + \frac{\sin^2 2\theta}{2} \right) + (\Psi_4 - \Psi_8)(1-\nu)\sin^2 2\theta \qquad \text{C.12}$$

$$\Lambda_{13} = (\Psi_2 \sin^4\theta + \Psi_6 \frac{\sin^2 2\theta}{2})\phi; \quad \Lambda_{14} = \Psi_2 \sin^2\theta \cos^2\theta - \Psi_6 \frac{\sin^2 2\theta}{2} \qquad \text{C.13, C.14}$$

$$\Lambda_{15} = -\left(\Psi_2 \sin^2\theta \frac{\sin 2\theta}{2} + \Psi_6 \frac{\sin 4\theta}{4} \right)\phi; \quad \Lambda_{16} = \Lambda_{14}\phi^2 \qquad \text{C.15, C.16}$$

$$\Lambda_{17} = \Psi_2 \cos^4\theta + \Psi_6 \frac{\sin^2 2\theta}{2}; \quad \Lambda_{18} = -\left(\Psi_2 \cos^2\theta - \Psi_6 \frac{\sin 4\theta}{4} \right)\phi \qquad \text{C.17, C.18}$$

$$\Lambda_{19} = 2\Lambda_{15}\phi; \quad \Lambda_{20} = -\Psi_2 \sin 2\theta \cos^2\theta + \Psi_6 \frac{\sin 4\theta}{2}; \quad \Lambda_{21} = \left(\Psi_2 \frac{\sin^2 2\theta}{2} + \Psi_6 \cos^2 2\theta \right)\phi \qquad \text{C.19, C.20, C.21}$$

$$\Lambda_{22} = -(1-\nu)\sin 2\theta \left[\Psi_4 \sin^2\theta - \Psi_8 (\cos 2\theta + \sin 2\theta) \right] - 2\Psi_4 (\sin^2\theta + \nu \cos^2\theta) \qquad \text{C.22}$$

$$\Lambda_{23} = \Psi_8 (1-\nu)\sin 2\theta (\cos 2\theta + \sin 2\theta) - \Psi_4 [(3-\nu)\cos^2\theta + 2\nu \sin^2\theta] \qquad \text{C.23}$$

Appendix D

Coefficients $co_{i,j}$, $i, j = 1, 2, 3, \ldots$ in equations (19-20) are derived from linear problem of clamped-clamped Euler beam[27]:

$[co_1\ co_2\ \ldots] = [4.7300\ \ 7.8532\ \ 10.9956\ \ 14.1372\ \ 17.2788\ \ 20.4200\ \ 23.5619\ \ 26.7035\ \ldots]$